Modification of commercial UF membranes by electrospray deposition of polymers for tailoring physicochemical properties and enhancing filtration performances

Elizaveta Korzhova, Sébastien Déon, Zakaryae Koubaa, Patrick Fievet, Dmitry Lopatin, Oleg Baranov

Modification of commercial UF membranes by electrospray deposition of polymers for tailoring physicochemical properties and enhancing filtration performances

Elizaveta Korzhova[1], Sébastien Déon[1], Zakaryae Koubaa[1], Patrick Fievet[1], Dmitry Lopatin[2], Oleg Baranov[2]*

1-Institut UTINAM (UMR CNRS 6213),
Université de Bourgogne-Franche-Comté, 16 route de Gray, 25030 Besançon cedex, France

2- PhotoChem Electronics LLC, Goryachiy Kluch, Russia

Submitted to

Journal of membrane Science

2019

*** Corresponding author**:

E-mail: sebastien.deon@univ-fcomte.fr (S. Déon)

Tel: +33 3 63 08 25 81

Abstract

The main challenge for a widespread use of nanoporous membranes in the removal of ionic contaminants lies in the adjustment of their physicochemical properties to allow adequate ion rejection and mitigate fouling based on the targeted application. Most of the commercial membranes are negatively charged and their use is thus not necessarily relevant for divalent cation rejection. The main objective for researchers is therefore to provide novel tailored membranes by developing specific synthesis or modifying available membranes. It is proposed here to tailor physicochemical properties of a commercial low molecular weight cut-off ultrafiltration membrane by electrospray deposition of polyethylenimine (PEI) and polystyrene sulfonate (PSS). In this study, it is highlighted that, with adequate conditions, it is possible to adjust the charge of the membrane surface, which can reach values from -40 to +40 mV (compared with -20 mV for pristine membrane). Surface hydrophilicity has also been increased with a contact angle decreased from 60 to 30° with a PSS surface layer. In terms of filtration performances, it is shown that the permeation flux is not reduced by the electrospray deposition of polymer and can even be slightly enhanced in specific conditions. When polymer concentration is sufficient, the deposit is able to face the shear stress induced by cross-flow filtration, probably due to viscosity effect. The positive PEI surface layer leads to a strong enhancement in the rejection of divalent cations whereas that of divalent anions is notably decreased due to electrostatic interactions between the charge of divalent ions and that of the membrane. The weaker impact of electrostatic interactions on monovalent ions allows adjustment of the separation selectivity between cations and anions as well as between mono- and divalent ions. Finally, it is also demonstrated that rejection performances are mostly governed by the surface layer, even if the underlying deposit layers and membrane also have a non-negligible impact on ion rejection.

Keywords

Ultrafiltration membrane; electrospray deposition; layer-by-layer assembly; ion rejection; zeta potential; hydrophilicity.

I. Introduction

In the perspective of sustainable development and environmental conservation, membrane processes appear as growing technologies for water treatment and pollution removal [1]. Indeed, they exhibit several advantages compared to other technologies due to low energy requirements, weak detrimental impact on environment, easy implementation, and high separation selectivity between components. Therefore, they currently represent one of the most viable options to remove a broad range of contaminants from polluted waters due to the wide variety of processes and materials available. For instance, membrane processes are a competitive technique to remove ionic or ionizable contaminants from polluted wastewaters by combining both steric effects and electrostatic interactions [2, 3].

Unfortunately, commercial membranes are often inadequate for particular applications, especially for removing multivalent cations such as heavy metals [4]. Moreover, their fouling also turns out to be a major drawback, impeding large-scale implementation [5, 6]. To overcome these issues, the development of specific membranes with adapted structural or physicochemical properties has become a key challenge for the expansion of membrane technologies. The target objective is to impart antifouling and/or antibacterial properties, and to obtain the best trade-off between permeability and separation selectivity [7-9]. This goal can be achieved by either synthesizing more effective membranes (containing mixed polymers or additives) [10-15] or improving surface properties through chemical or physical modifications (coating, grafting, etc…) [16-19]. Modifying commercial membranes by coating them with polyelectrolytes (charged polymers) seems to be a relevant way but usual methods show some drawbacks and the development of new modification methods remains a challenge for the membrane community.

Lots of routes are available in literature for surface coating (*e.g.* dip-coating [20, 21], spin-coating [22, 23], dynamic coating [24-26], electrodeposition [27, 28]) but dip-coating is often chosen due to its easy implementation. The latter, which consists in immersing the pristine membrane in a

82 polymer solution, is often used but its potential use for industrial application is impeded by the
83 large volume of polymer solution required for membrane immersion [29]. Spray deposition is an
84 alternative way to reduce polymer quantity and deposition time [30, 31]. However, its use is often
85 restricted to loading nanoparticles onto membrane surfaces [32-34].
86 In this study, the original technique of electrospray (ES) is proposed to deposit a small quantity
87 of polymer on the membrane surface. The electrospray deposition is a common technique which,
88 up to now, has not often been used for membrane modification [35]. With this technique, fine
89 droplets of polymer solution are sprayed on the membrane surface under a high voltage between
90 the needle containing the solution and the metallic support on which the membrane is stuck. The
91 advantages of this process lie in the small quantities of polymer that are coated on the membrane
92 surface (compared with immersion technique) and the inhomogeneous dispersion of the polymer
93 at the surface. In this study, two commercial membranes were modified by deposition of two
94 polyelectrolytes, namely polyethyleneimine (PEI) and polystyrene sulfonate (PSS). The impact
95 of various deposits obtained for various volumes and concentrations of sprayed polymer
96 solutions, was investigated on filtration performances, such as permeation flux, ion rejection and
97 separation selectivity, and discussed in terms of surface charge and hydrophilicity.
98

2. Material and methods

2.1. Membrane and solutions

Impact of polymer electrospray deposition was investigated on two ultrafiltration commercial flat-sheet membranes: a PLEIADE polyethersulfone (PES) membrane supplied by Orelis Environnement SAS (France) and a Desal GK thin film composite (TFC) membrane made up of a polyamide (PA) ultrathin layer on a polysulfone support (PS) supplied by GE Water & Process Technologies (Trevose, USA). Properties of the two membranes are summarized in Table 1.

Table1: Properties of the two investigated membranes

Membranes	MWCO* (Da)	Maximum pressure* (bar)	Wet thickness** (µm)	isoelectric point**	mean pore radius** (nm)	Intrinsic Permeability ** (m)
Pleiade	3000	5	190	3.4	2.5	8.4×10^{-14}
Desal GK	3000***	27	135	4.5	1.8	6×10^{-15}

* provided by supplier
** assessed during this study
*** Molecular weight cut-off was provided by supplier, but the value seems notably overestimated

Solutions were prepared by dissolving the organic and mineral solutes in ultrapure water (18.2 MΩ/cm). All experiments were carried out at the natural pH of water, namely 5.7 ± 0.2.

The two polymers used for deposition were polyethylenimine (PEI, branched) with a molecular weight of ~25,000 and polystyrene sulfonate (poly(sodium-p-styrene sulfonate), PSS) with a molecular weight of 70,000, which were purchased from Sigma-Aldrich (USA) and Acros organics (USA), respectively.

Deposition was carried out by spraying various volumes of polymer solutions. The polymer concentration was varied from 1.5×10^{-2} to 1.5 mol/L of functional groups (*i.e.* amino and carboxyl groups, respectively for PEI and PSS).

Concentrations of 10^{-3} mol/L for single salt solutions (namely NaCl, $MgCl_2$ and Na_2SO_4) and 5×10^{-4} mol/L for salt mixtures were chosen. Salts were supplied by Fisher Scientific, UK. Salt

and sucrose concentrations were estimated by ionic chromatography 883 Basic IC Plus (Metrohm) and refractometer RFM970-T (Bellingham & Stanley, supplied by Xylem Analytics), respectively.

2.2. Electrospray deposition

The modification of membrane properties was obtained by coating a small amount of polymer solution (PEI or PSS) on the surface by electrospray deposition. This technique, which was accurately described in literature [36], consists in spraying fine droplets of polymer solution by applying an electric current between a needle containing the polymer solution and a metallic support on which the membrane is stuck. The setup used in this study for deposition is depicted in Fig. 1.

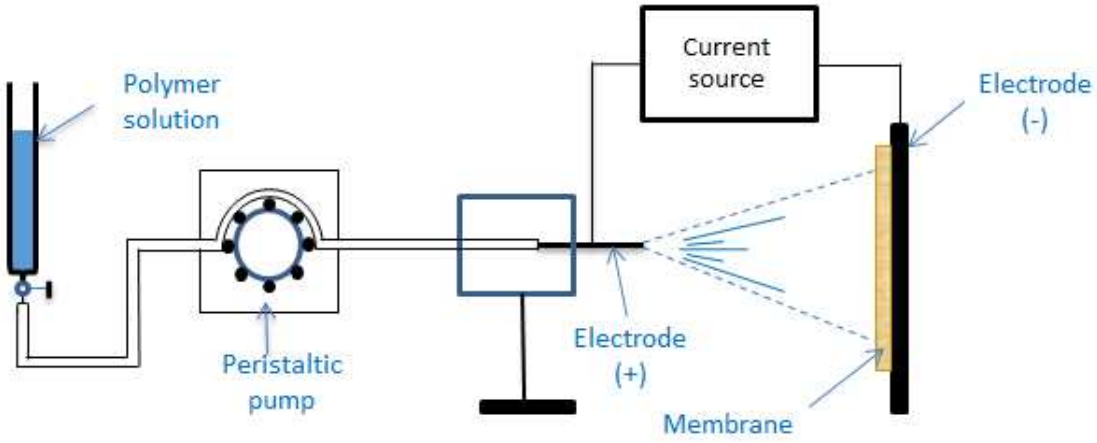

Fig. 1: Scheme of the setup used for electrospray deposition

Polymer is firstly dissolved in aqueous solution. The polymer solution is pushed into a metallic needle at a constant flow rate by a peristaltic pump. An electrical field is generated by a high-voltage regulated DC current source (XP Power Q101-5) between the needle and an aluminum plate (100 cm^2 area) used as counter electrode. The distance between the needle tip and the grounded target is 7 cm, the applied voltage was varied from 7 to 12 kV, and the flow rate was 1 mL/min. Deposition was carried out at ambient temperature. The needle and thus the spray

141 can be moved to cover all the membrane surface and the duration of spraying is calculated
142 according to membrane area, *i.e.* 140 cm^2 for filtrations and 30 cm^2 for characterizations (IR,
143 electrokinetic, contact angle measurements).

144 In order to determine the optimal conditions, the influence of sprayed volume and concentration
145 of monomer unit (amine or sulfonate groups) was investigated in the ranges of 5-50 $\mu L/cm^2$
146 and 0.15-1.5 mol/L, respectively.
147 Membranes were firstly immersed in a solution of KCl 10^{-3} mol/L before being coated by
148 spraying alternatively positively charged polymer (PEI) and negatively charged polymer PSS
149 (*i.e.* PEI, PSS/PEI and PEI/PSS/PEI) so that electrostatic attraction enables adhesion of the
150 sprayed layer on the previous layer (*i.e.* previously coated polymer or negatively charged
151 membrane surface). Membrane always remains wet and no drying step is implemented, so that
152 polymer remains dissolved during all the procedure.

153 ### *2.3. Filtration experiments*

154 A cross-flow lab-scale pilot was used in this study for ultrafiltration of solutions by flat-sheet
155 organic membrane. Flow rate is induced by a volumetric pump whereas transmembrane
156 pressure is generated by partially closing a regulation valve. Experiments were carried out in
157 full recycling mode (both permeate and retentate streams) to maintain feed concentration
158 constant and avoid variation of performances over time [37]. Circulation of cold water within
159 the feed tank jacket was used to set temperature at 25 ± 1°C. Filtrations were carried out at three
160 applied pressures (5, 15 and 25 bar) but results are provided here only for ΔP = 15 bar in order
161 to minimize experimental data and simplify graphs. It was not possible to duplicate each
162 measurement and error bars cannot therefore be displayed. However, few experiments were
163 repeated to validate the reproducibility, and discrepancies were lower than 5%. Moreover, it
164 should be mentioned that experiments before and after modification were always carried out
165 with the same membrane sample to overcome discrepancy between membrane sheets.

166 Performances obtained with pristine and modified membranes were estimated by calculating
167 permeation flux J_v and ion rejection R_i with Eqs. 1 and 2 from the mass of permeate m_p measured
168 during a filtration time Δt and feed $C_{i,f}$ and permeate $C_{i,p}$ concentrations.

169 $$J_v = \frac{m_p}{\Delta t \ \rho \ S_m} \quad (1)$$

170 $$R_i = 1 - \frac{C_{i,p}}{C_{i,f}} \quad (2)$$

171 where S_m is the membrane area and ρ the solution density.

172 ## *2.4. Membrane characterization*

173 ### *2.4.1. Zeta potential measurements*

174 ζ-potential of the external surface was measured before and after polymer spraying by
175 Tangential Streaming Current (TSC) measurements, which were carried out with a ZetaCAD
176 zetameter supplied by CAD Inst. The principle and setup were already accurately described in
177 previous papers [38]. Briefly, nitrogen gas is injected in the feed tank, which leads to flow of
178 the electrolyte solution (KCl 10^{-3} mol/L) across a rectangular channel made by two identical
179 membranes facing each other. A pressure drop through the channel ΔP is induced by this flow.
180 Additionally, excess of counter-ions within the diffuse layer is carried by the solution flow
181 generating a streaming current I_s, which is measured by two Ag/AgCl wire electrodes for each
182 pressure drop. The slope of $I_s = f(\Delta P)$ can then be used to estimate the ζ-potential value by Eq.
183 3, provided that the channel geometry is known [39]:

184 $$\varsigma = \left(\frac{l_c}{h_c L_c} \right) \frac{\eta}{\varepsilon_0 \varepsilon_r} \times \left(-\frac{I_s}{\Delta P} \right) \quad (3)$$

185 with l_c, L_c and h_c the channel length, width and height, respectively, and η, ε_0 and ε_r the dynamic
186 viscosity, vacuum permittivity and the dielectric constant of the solution.

187

188 ***2.4.2. Surface hydrophilicity estimation***

189 Variation of the membrane surface hydrophilicity was estimated by contact angle
190 measurements. On each sample, 20 drops of ultrapure water were placed at different positions
191 on the dry membrane surface at ambient temperature. Images obtained with a digital video
192 camera were processed using computer program and contact angles were measured 10 seconds
193 after applying the drop. Then, average values and standard deviation were calculated for
194 discussion.

195 ***2.4.3. Surface chemical analysis***

196 The surface of the membrane before and after deposition was chemically investigated by
197 attenuated total reflection - Fourier transform infrared (ATR-FTIR) spectroscopy. A FTIR
198 spectrometer iS50 (Thermo Scientific) with ATR attachment VarigATR (Harrick) were used
199 with an angle of 65° and spectra were acquired in the spectral region between 800 and
200 4000 cm^{-1} with 2 cm^{-1} resolution.

201 ***2.4.4. Morphological analysis***

202 The morphology (roughness) of membrane surface was investigated by AFM. Images of
203 membrane surface (with and without deposition of PEI and PSS) were performed in contact
204 mode with the commercial Nano Observer atomic force microscope from CSI (France). The
205 treatment of AFM pictures and roughness assessment were performed using MoutainsMap®
206 software from Digital Surf.

207 Images of the membrane cross section were obtained by Scanning Electron Microscopy (SEM)
208 after Focused Ion Beam (FIB) irradiation. To avoid charge accumulation on the surface, the
209 membrane surface was covered with a chromium layer of 20 nm by cathodic sputtering. The
210 membrane surface was irradiated by the focused Ga^+ ions (FIB Orsay-Physic with ionic column
211 CANION 31). After this irradiation step, the cross-section was observed by SEM (Gemini
212 Column, Zeiss) with a tilt of 50°.

2.4.5. Structural characterization

Membrane intrinsic permeability and mean pore radius were estimated from filtration of pure water and neutral solutes, namely sucrose and PEG 2000 for Desal GK and PLEIADE membranes, respectively.

Membrane intrinsic permeability L_p was assessed from pure water flux $J_w = f(\Delta P)$ by Darcy's law:

$$J_w = \frac{L_p}{\eta}\Delta P \tag{4}$$

L_p is therefore a structural property since viscosity is not included in this parameter. Hence, considering a laminar flow in cylindrical pores, Hagen-Poiseuille equation can be coupled with Darcy's law to obtain the expression of L_p:

$$L_p = \frac{\varepsilon r_p^2}{8L} \tag{5}$$

A change in membrane intrinsic permeability can be imputed to variations in mean pore radius r_p, porosity ε or pore length L (*i.e.* membrane thickness if tortuosity is neglected).

Mean pore radius is estimated by fitting rejection curves $R = f(J_v)$ with a steric hindrance model [40, 41] (Eqs. 6, 7, 8) for which, mean pore radius is the only adjustable parameter, diffusivities at infinite dilution $D_{i,\infty}$ and Stokes radius $r_{i,s}$ of neutral solutes being retrieved from literature.

$$R = 1 - \frac{\phi_i K_{i,c}}{1 - \left[\left(1 - \phi_i K_{i,c}\right) \left(\exp\left(-\frac{K_{i,c}\Delta P}{8 K_{i,d} D_{i,\infty} \eta} r_p^2\right) \right) \right]} \tag{6}$$

where ϕ_i, $K_{i,c}$, $K_{i,d}$ are the steric partitioning coefficient, and convection and diffusion hindrance factors, respectively, calculated by [42]:

$$\phi_i = \left(1 - \frac{r_{i,s}}{r_p}\right)^2 = \left(1 - \lambda_i\right)^2 \tag{7}$$

$$K_{i,c} = (2 - \phi_i)(1 + 0.054\lambda_i - 0.988\lambda_i^2 - 0.441\lambda_i^3) \tag{8}$$

234 $$K_{i,d} = 1 - 2.30\lambda_i + 1.154\lambda_i^2 + 0.224\lambda_i^3 \quad (9)$$

235

3. Results & Discussion

3.1. Influence of electrical field

Electrospray deposition technique requires a high voltage, which can potentially have an influence on the membrane polymer. In a first step, the influence of the electrical field on membrane was investigated by spraying only water, so that modification of membrane performances cannot be attributed to deposition. The applied voltage was chosen at 12 kV and the impact was studied by estimating the rejection R and permeation flux J_v of salts and neutral solutes (*cf.* Fig. 2) as well as intrinsic permeability L_p and mean pore radius r_p (*cf.* Table 1), obtained with PLEIADE and GK membranes before and after water electrospray.

From Fig. 2, it can be seen that permeation fluxes obtained with PLEIADE membrane clearly decrease after spraying water, which cannot be attributed to any deposit. Rejection of salts was not significantly impacted except that of Na_2SO_4, which was slightly increased by electrospray. Oppositely, electrical field involved in electrospray of water seems to enhance flux of Desal GK membrane, whereas rejection is not noticeably affected, except a very slight increase in NaCl rejection.

The rejection of salts is governed by both steric and electric mechanisms. The fact that salt rejection is not impacted tends to show that membrane charge is probably not strongly affected by electrical field. The large size of SO_4^{2-} ion compared with other ions can probably explain the slight increase of its rejection due to a stronger steric exclusion. Flux and rejection of neutral solutes are mainly governed by structural properties. The values of intrinsic permeability L_p and the mean pore radius r_p, estimated by fitting pure water flux and rejection of neutral solutes (PEG 2000 for PLEIADE membrane and Sucrose for Desal GK) with Eqs. 4 and 6, before and after water electrospray, are provided in Table 2 for deeper discussion.

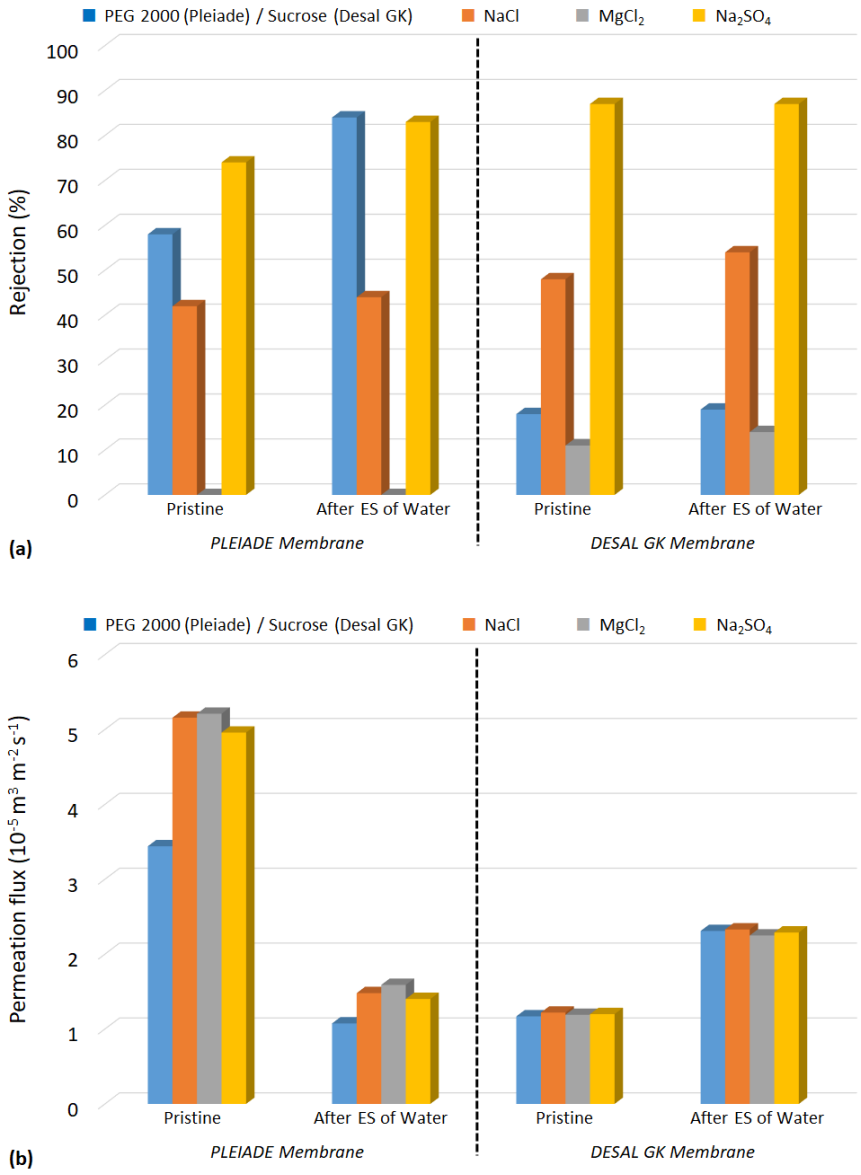

Fig. 2: Rejection (2a) and permeation flux (2b) of salts and neutral solutes obtained with PLEIADE and GK membranes, before and after electrospray of water with a voltage of 12 kV

Table 2 demonstrates that structural properties of the PLEIADE membrane (mean pore radius and intrinsic permeability) are clearly affected by the application of an electrical field through the membrane, whereas only permeability seems to be impacted for the GK membrane. Indeed, intrinsic permeability of PEIADE membrane was decreased by 60% and mean pore radius by almost 30% because of the electrical field applied for spraying solutions. This means that the PES constituting this membrane is probably damaged by the technique. Indeed, the electric field may cause local temperature increase, which could expand membrane polymer and therefore

lead to a decrease of mean pore size (increase in PEG rejection) and permeation flux. Oppositely, the polyamide of the Desal GK is positively affected by electric field since an increase in intrinsic permeability is observed. However, the mean pore radius after water electrospray is unchanged. Considering the expression of intrinsic permeability (Eq. 5), the increase in permeability induced by electric field can be attributed to an increase in porosity or a decrease in membrane thickness. It is perhaps possible that the electrical field passing through the membrane leads to the creation of additional pores within the active layer (without changing the mean pore size) and/or the shrinkage of this thin layer.

In any case, the aim of this study being to optimize filtration performances, the rest of this study has been implemented only with Desal GK membrane in order to exploit the positive impact of electric field on its performances. Similar trends (but to a lesser extent) were obtained at 7 kV for both Desal GK and Pleiade membranes, and it was thus chosen to work with this lower applied voltage in order to minimize its impact and ensure that variations are mainly due to polymer deposits. All the following results were thus obtained with an applied voltage of 7 kV.

Table 2: Intrinsic permeability L_p and mean pore radius r_p of the two investigated membranes, before and after electrospray of water with a voltage of 12 kV.

Membrane	**PLEIADE**		**DESAL GK**	
	Pristine	After water ES	Pristine	After water ES
L_p (10^{-14} m)	8.4	3.3	0.6	1.2
r_p (nm)	2.5	1.8	1.8	1.8

3.2. Deposit highlighting

Before studying the influence of electrospray conditions, the presence of deposit was checked by attenuated total reflection – Fourier-transform infrared (ATR-FTIR) spectroscopy, and SEM and AFM images. The FTIR spectra obtained with pristine membrane and membrane modified by PEI and PSS/PEI depositions are given in Fig. 3.

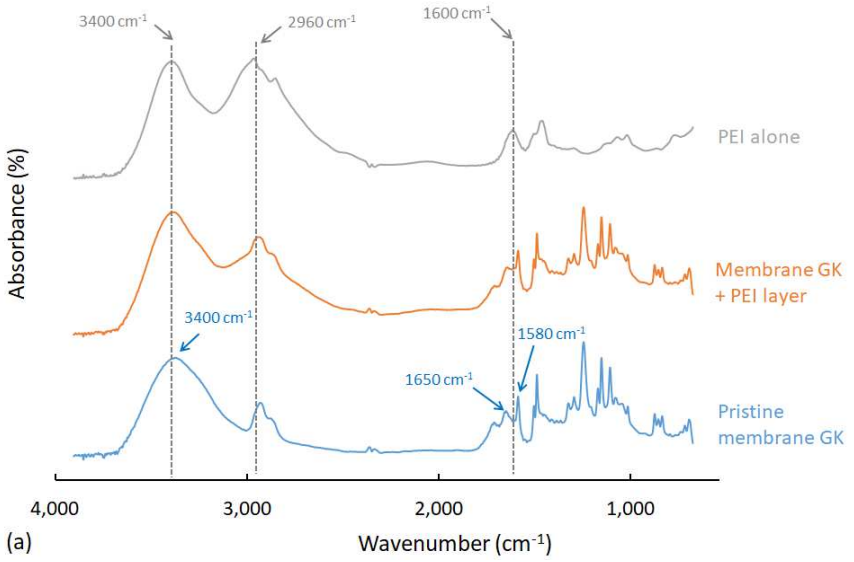

295

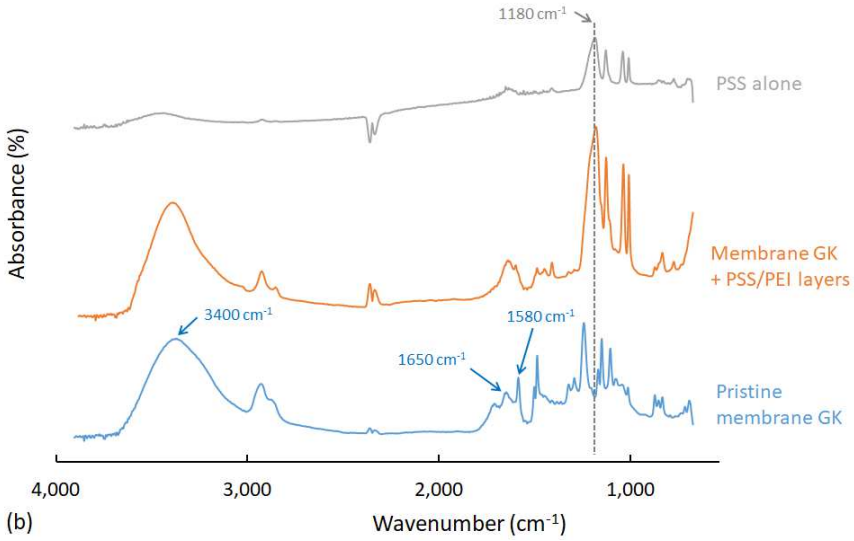

296

297 **Fig. 3**: FTIR spectra of pristine and modified membrane surfaces, as well as polymers alone, for
298 electrospray deposition of a PEI layer (3a) and PSS/PEI layers (3b).

299 The usual peaks characteristic of polyamide polymer obviously appeared in the spectra of
300 pristine membrane. For instance, the bands at 3400, 1650 and 1580 cm^{-1} refer to the stretching
301 of N–H, stretching of C=0, bending of N–H bonds of the amide group, respectively. Bands
302 characteristic of amine groups of PEI, namely stretching of N–H, stretching of N–H (amine
303 salt) and bending of N–H appear at wavelength of 3400, 2960 and 1600 cm^{-1}, respectively.
304 These bands are also observable on the spectra of pristine and modified membranes (in Fig. 3a),
305 which can be explained by the similarity of amide and amine groups. Moreover, it is likely that

306 the pristine membrane contains residues of amine groups from polymerization process, which
307 is suggested by the band referring to stretching of N–H (amine salt) at 2960 cm^{-1} (Fig. 3a). This
308 can explain why specific bands of amine groups from PEI are not discernible on modified
309 membrane by electrospray of PEI. Oppositely, the specific band referring to stretching of S=O
310 of sulfonate group from PSS (which appears at 1180 cm^{-1} in Fig. 3b) can be observed on the
311 spectrum of the membrane modified by PSS/PEI, whereas this band does not appear on the
312 spectrum of pristine membrane. The presence of this specific band of PSS (and others) clearly
313 proves that the PSS was deposited on the PEI layer. Hence, this also shows that PEI was coated
314 on membrane surface, even if its presence was not demonstrated from FTIR spectra.
315 To conclude, FTIR study clearly demonstrates the effective coating of membrane surface by
316 polymers during electrospray.
317 Fig. 4 presents the surface morphology obtained by AFM images and membrane cross-section
318 observed by FIB-SEM for pristine membrane (a, b) and after PEI (c, d) and PSS/PEI (e, f)
319 electrospray depositions. The corresponding values of roughness and thickness of the active
320 layer alone or with PEI and PSS/PEI deposits are summarized in table 3.

321
322 Table 3. Arithmetical mean height (S_a), root mean square height (S_q) and layer thickness of the
323 pristine membrane and membrane modified by electrospray deposition of PEI and PSS/PEI.

Membranes	S_a (nm)	S_q (nm)	Thickness (nm)
Active layer of pristine membrane	4.0	5.0	80
Active layer + PEI deposition	3.6	4.6	130
Active layer + PSS/PEI deposition	4.4	5.6	470

324
325

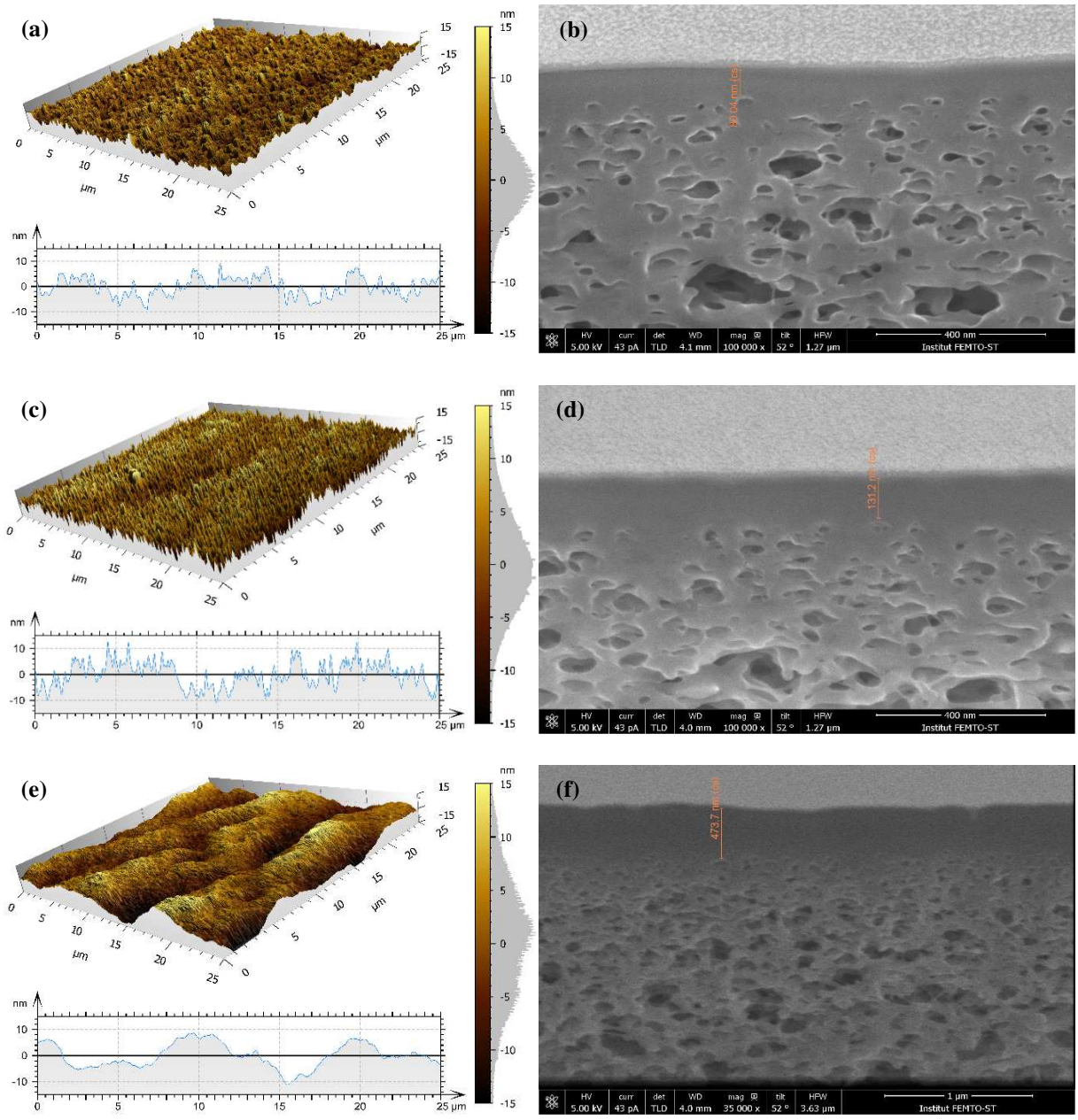

Fig. 4: AFM images of membrane surface (a, c, e) and membrane cross-section observed by FIB-SEM (b, d, f) for pristine membrane (a, b), and after electrospray deposition of PEI (c, d) and PSS/PEI (e, f).

AFM images provided in Fig. 4 (a, c, e) show that PEI deposition seems to have a weak impact on roughness and surface morphology. The roughness is identical and only a few tightening of peaks and valley is observable. Oppositely, the terminating layer of PSS (i.e. PSS/PEI deposition) was found to strongly modify surface morphology. Indeed, with this bi-layer deposit, the surface is smoother even if roughness remains similar, and the unevenness is more spread leading to larger peaks and valleys.

SEM images of the membrane cross-section (Figs. 4b, 4d, 4f) show that the thickness of the thin surface layer (given in Table 3) slightly increases when PEI is sprayed (from 80 to 130 nm). When a PSS terminating layer is deposited on the PEI layer, the thickness is largely increased up to 470 nm. This confirms that PEI layer have a weak impact on membrane structure, whereas PSS deposit strongly modify the morphological properties of the overall membrane.

3.3. Influence of spray parameters on membrane physicochemical properties

It is known that hydrophilicity is an important property of UF membranes, which tends to increase permeation flux but also reduce its fouling by various hydrophobic pollutants. So, the impact of the polymer deposition on hydrophilicity was investigated by contact angle measurements on the pristine and the PEI-modified membranes. Similarly, ion rejection and separation selectivity are governed by electrostatic interactions between the charge of ions and that of membrane surface. Hence, the impact of polymer deposition on the value of ζ-potential was also investigated, which was estimated by tangential streaming current measurements.

3.3.1. Influence of sprayed volume / spray duration

The main asset of electrospray deposition lies in the small quantities of polymer solution required for coating. However, the volume of sprayed solution can have an influence on surface properties. The sprayed volume of PEI solutions was varied from 2.5 to 50 µL/cm^2 and the impact on both contact angle and ζ-potential was investigated. Each volume was sprayed at a constant flow-rate of polymer solution (3×10^{-1} mol L^{-1} of PEI amine group), which was fixed at 1 mL/min. The duration of pulverization was also dependent on the membrane sample area. Evolution of contact angle and ζ-potential for the various sprayed volumes is provided in Fig. 5.

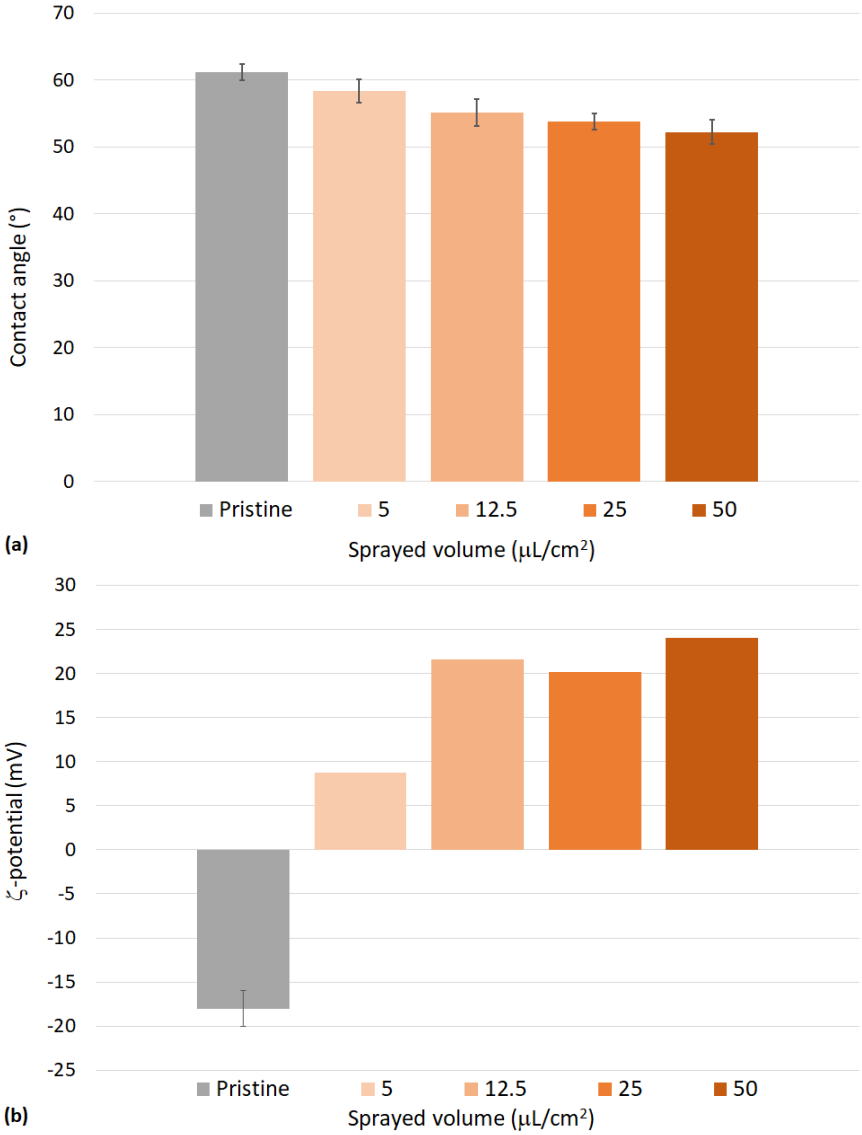

Fig. 5: Evolution of the surface contact angle (5a) and ζ-potential (5b) with the volume of sprayed solution containing 3×10^{-1} mol L^{-1} of PEI

Fig. 5a shows that the contact angle between the water drop and the surface decreases monotonously when the volume of sprayed polymer solution increases. This means that the deposit of PEI makes the surface more hydrophilic, which can have a positive impact on flux and membrane fouling. The fact that contact angle seems to decrease more slightly for sprayed volumes larger than 12.5 µL/cm^2 tends to show that the membrane is probably partially covered by PEI for low sprayed volumes. It should be noted that this decrease in hydrophobicity is moderated, probably because PEI is slightly more hydrophilic than membrane surface, the hydrophilic properties of which come from exposed polar amine groups.

ζ-potential values given in Fig. 5b confirm the presence of a PEI deposit at the membrane surface, which allows a reversal of the sign of the surface charge, as illustrated in literature [43]. From Fig. 5b, it can be observed that the membrane surface becomes positive after electrospray deposition of PEI and the positive charge is higher when the volume of sprayed solution is larger. It should be stressed that for volumes higher than 12.5 µL/cm^2, the membrane charge no longer seems to be affected by the sprayed volume since differences in zeta potential from 12.5 to 50 µL/cm2 are within the confidence interval, which was assessed with several pristine membranes. This trend suggests that the membrane surface is probably almost covered by polymer above this volume.

3.3.2. Influence of polymer concentration

The influence of PEI concentration was investigated on both contact angle and ζ-potential values. The evolutions with concentration of monomer unit of PEI (amine groups) are provided in Fig. 6 for a sprayed volume of 50 µL/cm^2.

Fig 6 shows that polymer concentration also plays a major role on both surface hydrophilicity and electrical properties. It even seems that the impact of concentration is more striking than that of sprayed volume. For instance, contact angle is found to monotonously decrease when concentration of PEI increases up to 45° for a concentration of 15×10^{-1} mol/L of PEI monomer unit. It can be seen in Fig. 6b that a too low amount of polymer does not allow a reversal of the charge sign ($C < 0.75 \times 10^{-1}$ mol/L) but tends to decrease the negative charge. For concentrations higher than 0.75×10^{-1} mol/L, the positive charge monotonously increases with concentration, up to 45 mV, without reaching a plateau. It should be noted that for concentrations higher than 15×10^{-1} mol/L, the high viscosity of polymer solution clearly complicates the pulverization.

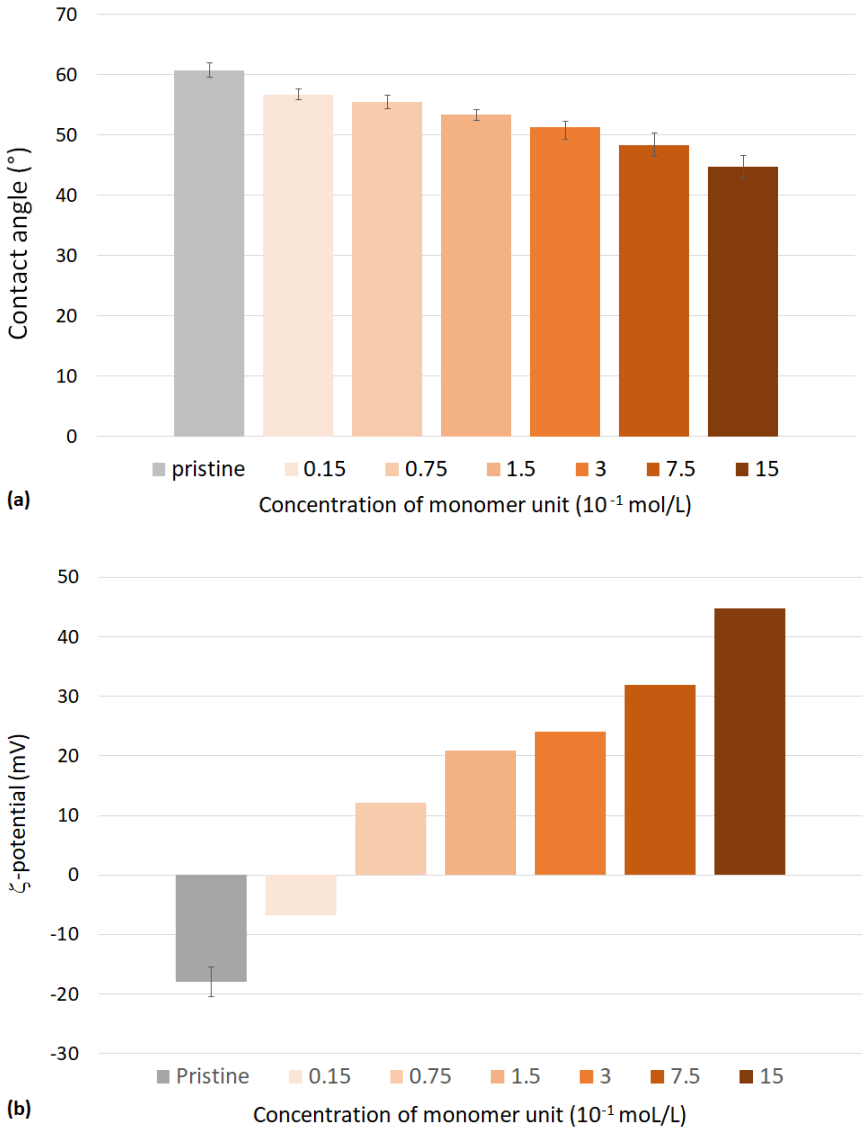

Fig. 6: Evolution of the surface contact angle (6a) and ζ-potential (6b) with the concentration of PEI monomer unit for a sprayed volume of 50 µL/cm^2

These trends are consistent with literature in which it was already highlighted that a higher polymer concentration leads to larger polymer deposition rates, which obviously results in more polymer adsorption on the membrane surface [44]. These outstanding modifications of physicochemical properties with electrospray deposition of PEI should have a notable impact on filtration performances.

3.4. Impact of PEI electrospray deposition on filtration performances

The main aim of PEI deposition is to increase electrostatic interactions between divalent ions

and membrane surface. Hence, the impact of the PEI concentration on filtration performances is firstly investigated on $MgCl_2$ and Na_2SO_4 rejections. A salt concentration of 10^{-3} mol/L was chosen for filtration to keep a low ionic strength and avoid the screening of electrostatic interactions between PEI and membrane surface as well as between PSS and PEI. Indeed, at high ionic strength, charges of polyelectrolytes become neutralized by salt counter-ions, which leads to weaker electrostatic attraction and results in thicker modified layers [45].

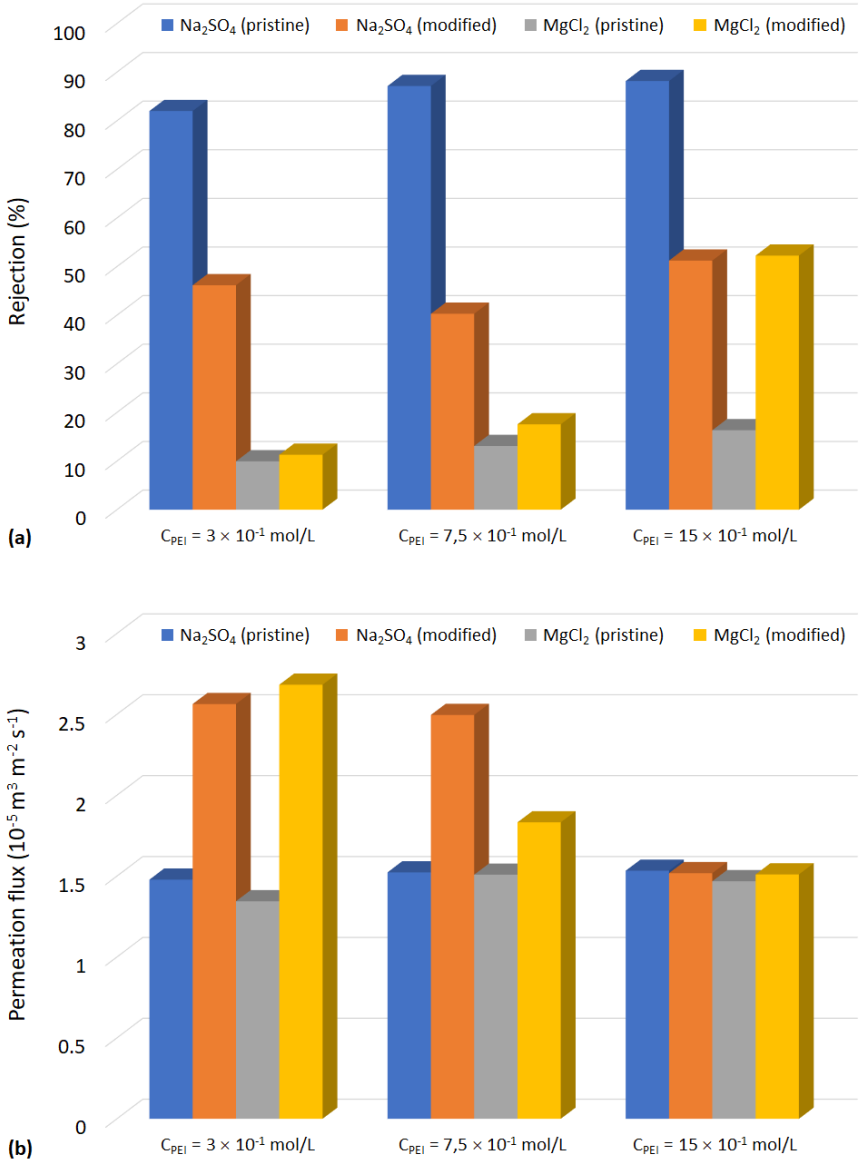

Fig. 7: Rejection (7a) and permeation flux (7b) at 15 bar of $MgCl_2$ and Na_2SO_4 measured with both pristine and modified membranes for three concentrations of PEI monomer units $\{V_{sprayed} = 12.5\ \mu L/cm^2\}$

Salt rejection by pristine and modified membranes measured at 15 bar are provided for the three highest concentrations of PEI monomer unit in Fig. 7. The volume sprayed was chosen at 12.5 $\mu L/cm^2$ (beginning of the plateau for ζ-potential) to limit the quantity of polymer at the membrane surface and its potential impact on permeation flux.

It can be observed in Fig. 7a that electrospray deposition of PEI has a different impact on the rejections of divalent cations and anions. Indeed, a sharp decline of sulfate rejection is obtained irrespective of the PEI concentration in the sprayed solution. Unlike many studies found in literature [43], magnesium rejection is almost not enhanced, until a high concentration of PEI is sprayed. This means that the quantity of polyelectrolyte is enough to screen the primitive negative charge of the membrane but not enough to induce a strong repulsive interaction between positive PEI coated at the membrane surface and divalent cations. This conclusion is not in accordance with the values of zeta-potential provided in Fig. 6b since it seems that membrane surface charge is strongly positive even for lower PEI concentrations. In fact, this unexpected behavior can probably be explained by the high shear stress condition induced by cross-flow filtration, and especially with spacer-filled retentate channel, compared with the smoother laminar conditions occurring during streaming current measurements. It was shown in literature that a transition to unsteady flow occurs at relatively low Reynolds numbers ($Re < 50$) in spacer-filled channels. Indeed, spacer acts as a turbulence promoter leading to the development and separation of boundary layers, vortices formation, creation of high shear regions and recirculation zones [46], which obviously tends to break down deposits. Hence, it seems that the electrostatic interactions between the membrane and PEI are probably not sufficient to keep the whole deposit at the membrane surface under these harsh conditions. Harsh conditions are few investigated in studies reported in literature for which most of filtrations are implemented in dead-end mode [47, 48] or with smoother cross-flow conditions [49, 50]. However, for a high concentration such as 15×10^{-1} mol/L of monomer unit, the strong

447 increase in solution viscosity probably leads to stronger adhesion of the polymer and a decrease
448 of Reynolds values, which makes it more relevant for real cross-flow conditions.
449 A cross-linking procedure leading to covalent bonds would probably have enhanced the
450 stability of PEI coating, especially with high salt contents for which electrostatic interactions
451 are screened.
452 Concerning the performances in terms of permeation, it can be concluded from Fig. 7b that the
453 flux increases after electrospray deposition, as it was previously observed with water spray.
454 However, this increase was found to be progressively reduced when PEI concentration
455 increases. This trend can be attributed to the accumulation of polymer at the membrane surface,
456 which obviously tends to increase overall membrane resistance to permeation. At 15×10^{-1}
457 mol/L, the increase in permeability induced by electrospray is fully balanced by the presence
458 of the coated polymer layer and the resulting permeation flux is therefore not impacted by the
459 modification compared with pristine membrane. This groundbreaking result is of prime
460 importance for a potential use since it was proved that this method allows an improvement of
461 cation rejection without negative impact on the permeation flux.
462 Enhancement in terms of divalent cation rejection was highlighted in this study. However,
463 treatment of real solution implies to investigate separation selectivity for ion mixtures that
464 mimic real-life conditions. To deeply investigate the impact of electrospray deposition on the
465 filtration performances with ionic mixtures, the rejection curves for ternary and quaternary ion
466 solutions are provided in Fig. 8 and 9 for the highest PEI concentration (15×10^{-1} mol/L of
467 monomer unit).

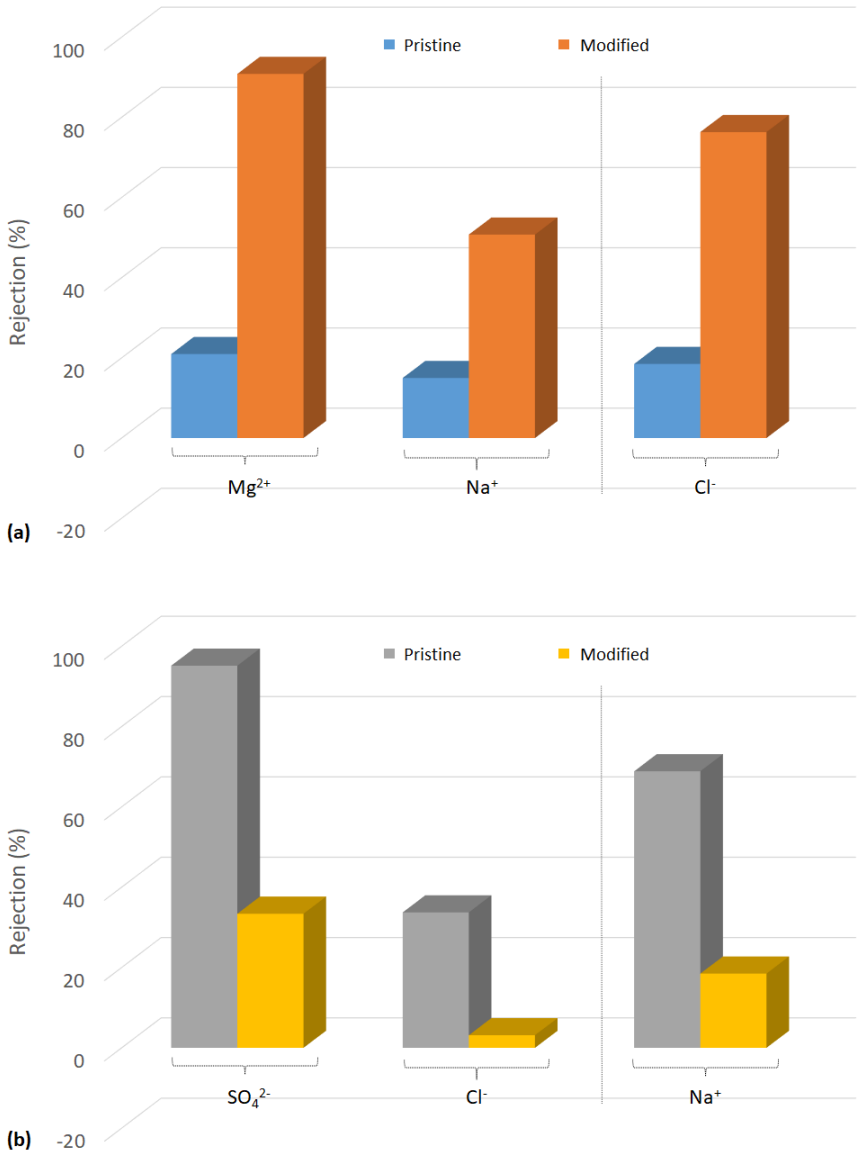

Fig. 8: Ion rejections at 15 bar for ternary mixtures (6a: $MgCl_2$-NaCl and 6b: Na_2SO_4-NaCl) measured with both pristine and modified membranes {$C_{PEI} = 15 \times 10^{-1}$ mol/L and $V_{sprayed} = 12.5$ µL/cm^2}

Trends observed with the single salt solutions are confirmed by curves obtained with ternary solutions. Indeed, it can be seen in Fig. 8 that the electrospray deposition of PEI clearly increases rejection of cations and more intensely that of divalent cations, which leads to a better selectivity between mono- and divalent cations. Similarly, rejection of anions and especially divalent anions are decreased by the PEI deposition, which leads to a strong decrease of the selectivity between mono- and divalent anions. It should be stressed that rejections of the common ion Cl^- for $MgCl_2$-NaCl mixture and Na^+ for Na_2SO_4-NaCl mixture are not relevant

for discussion since their variation is imposed by the two other ions and their value is always intermediate between mono- and divalent non-common ions, due to electroneutrality condition. These trends are highly valuable for the potential application of heavy metal removal. Electrospray deposition can be implemented to enhance the removal of multivalent metal ions (e.g. Cu^{2+}, Co^{2+}, Ni^{2+}, etc.) without retaining monovalent ions. Rejection of ions from quaternary mixtures (shown in Fig. 9) is also interesting but the impact of modification is less notable, and rejection must be compared at two concentrations to understand how modification govern selectivity of complex ion mixtures. Fig 9 provides the rejection of the four ions with the pristine membrane and the same membrane modified by spraying 7.5 and 15×10^{-1} mol/L of PEI monomer unit.

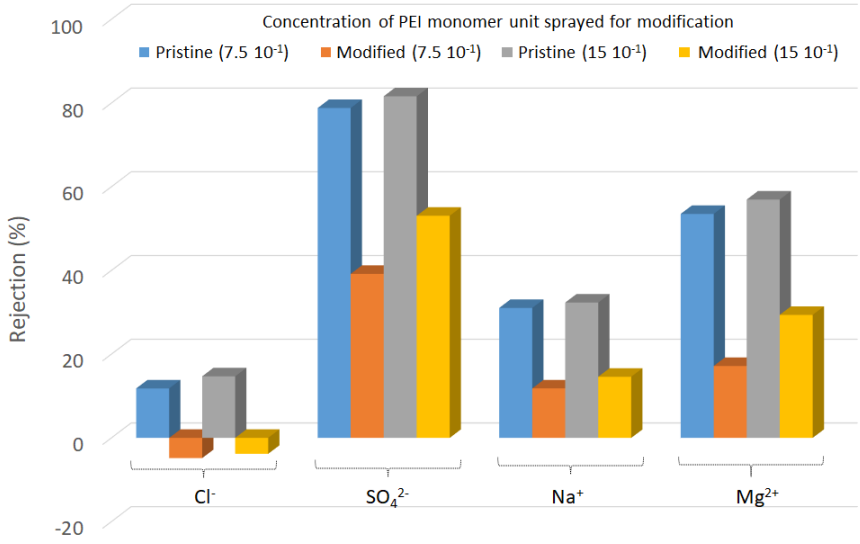

Fig. 9: Ion rejections measured at 15 bar before and after electrospray deposition of PEI at two concentrations of monomer unit {$V_{sprayed}$ = 12.5 µL/cm²}

From Fig. 9, it can be concluded that rejection of both anions and cations, and especially Mg^{2+} and SO_4^{2-}, decreases due to PEI deposition, which was unexpected considering results observed with ternary mixtures. However, it appears that SO_4^{2-} rejection strongly decreases due to the presence of polymer for 7.5×10^{-1} mol/L of PEI. This fall results in a strong decline of Mg^{2+} rejection due to electroneutrality condition, Na^+ and Cl^- being weakly impacted by

498 modification. In the case of the solution containing 15×10^{-1} mol/L of PEI monomer unit, it can
499 be seen that the changes in electrostatic interactions caused by PEI deposit tends to reduce the
500 decline of Mg^{2+} rejection (due to repulsion with positive PEI), thereby reducing the decline of
501 SO_4^{2-} rejection to comply with electroneutrality condition. In ion mixtures, the transport of the
502 monovalent anion is favored to balance the high rejection of divalent anion and the low rejection
503 of cations. Sulfate ion being highly rejected, the transfer of cations forces the transfer of
504 chloride ion to maintain electroneutrality, which can lead to negative rejections. It can be noted
505 that the very low monovalent rejections and especially the negative rejection of chloride
506 obtained after PEI electrospray are particularly attractive for applications that aim at enriching
507 oligo elements (multivalent ions) by desalting (NaCl removal) the retentate stream.

508 **3.5. Impact of layer-by-layer electrospray deposition**

509 Various layers were deposited by electrospray of polymer solution containing 15×10^{-1} mol/L
510 of monomer unit by alternating (positive and negative) polymers, *i.e.* PEI, PSS/PEI,
511 PEI/PSS/PEI. Indeed, layer-by-layer assembly is mainly driven by electrostatic interactions and
512 a negatively charged PSS layer cannot be coated on negative membrane surface. It should be
513 stressed that even if electrostatic interactions are the main forces governing layer-by-layer
514 assembly, it is not the sole mechanism and additional forces such as hydrophobic interactions
515 and entropy gain have an impact on deposition by restructuring and release of water molecules
516 and counter-ions [29].

517 ***3.5.1. Impact on surface properties***

518 The impact of layer-by-layer electrospray on contact angle and zeta-potential are provided in
519 Fig. 10.

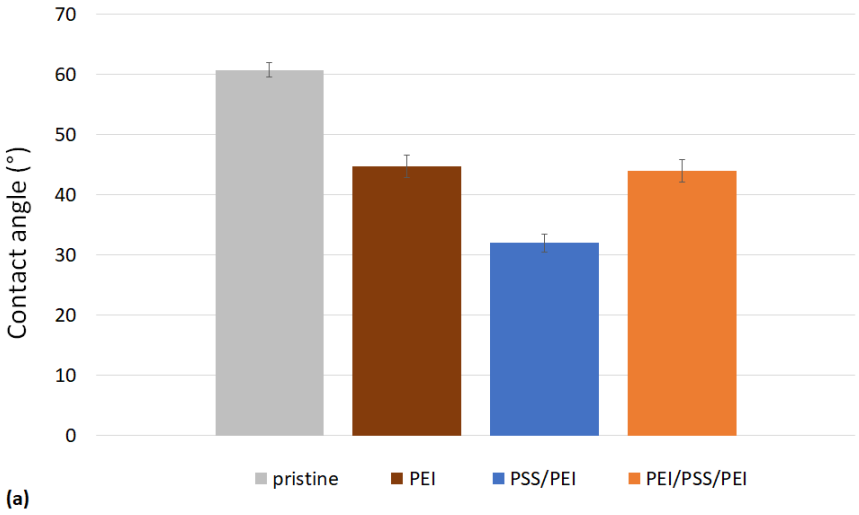

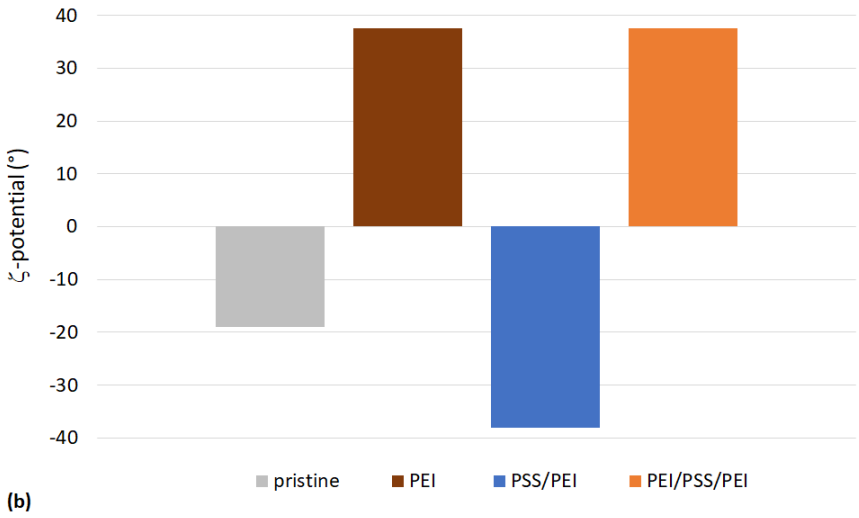

Fig. 10: Evolution of the surface contact angle (10a) and ζ-potential (10b) with the various deposited layers {$C_{PEI} = 15 \times 10^{-1}$ mol/L and $V_{sprayed} = 50$ µL/cm^2}

Fig. 10a shows that all deposits make the surface more hydrophilic than that of pristine membrane. It can also be seen that the PSS layer seems clearly more hydrophilic than the PEI layer. Hydrophilicity enhancement by PEI deposition can mainly be attributed to exposed polar amine groups at the membrane surface, whereas that obtained by PSS is induced by hydrophilic sulfonate groups. Contact angle of modified membrane surface is similar for terminating layers made of PEI when PEI is deposited either on PSS (*i.e.* PEI/PSS/PEI layers) or on membrane surface (PEI layer only). This means that the sublayers have a negligible impact on the

hydrophilicity of the modified membrane surface, confirming that the surface is almost fully covered by the various layers.

Values of ζ-potentials provided in Fig. 10b clearly show that it is possible to obtain positive or negative surface charge by alternatively spraying positive (PEI) and negative (PSS) polymers, as it was previously highlighted in literature with other polymers [51]. Spraying PSS on a PEI layer even leads to a more negative surface charge than that of the pristine membrane. Finally, the deposition of a second PEI layer on the PSS/PEI layers leads to the same membrane charge than that achieved with only one PEI layer.

Moreover, superimposing alternatively more than 1 layer of PEI and PSS does not seem to present a substantial interest in terms of physicochemical properties, even if some changes in growth mechanisms and selectivity performances with the number of layers have been already highlighted in literature [52].

3.5.2. Impact on filtration performances

Rejections and permeation flux obtained with pristine membrane and membranes modified by alternating PEI and PSS layers are provided in Fig. 11.

The filtration performances measured with various layers of PEI and PSS show that the external (terminating) layer mainly governs the rejection of salts. Indeed, the rejection of $MgCl_2$ is highly increased when PEI is the external layer (*i.e.* PEI or PEI/PSS/PEI) and in the same order of magnitude. Similarly, the rejection of Na_2SO_4 is strongly decreased in the latter case. These trends perfectly meet expectations and results provided in literature [53], and can be explained by electrostatic interactions. Oppositely, the rejection of $MgCl_2$ is slightly increased and that of Na_2SO_4 notably decreased when external layer is made of PSS. These impacts are surprising since it is expected that the higher negative surface charge of the membrane modified by PSS/PEI compared with pristine membrane (shown in Fig. 10b) should lead to a decrease in $MgCl_2$ rejection and an increase in Na_2SO_4 rejection. This could be explained by the fact that

rejection is probably not merely governed by the superficial layer but also partially by the deeper deposited sublayers and membrane body. This impact could perhaps also be attributed to the fact that the membrane surface is not fully covered when 12.5 µL/cm^2 of polymer solution is sprayed, some amino groups being available for electrostatic interactions with divalent ions.

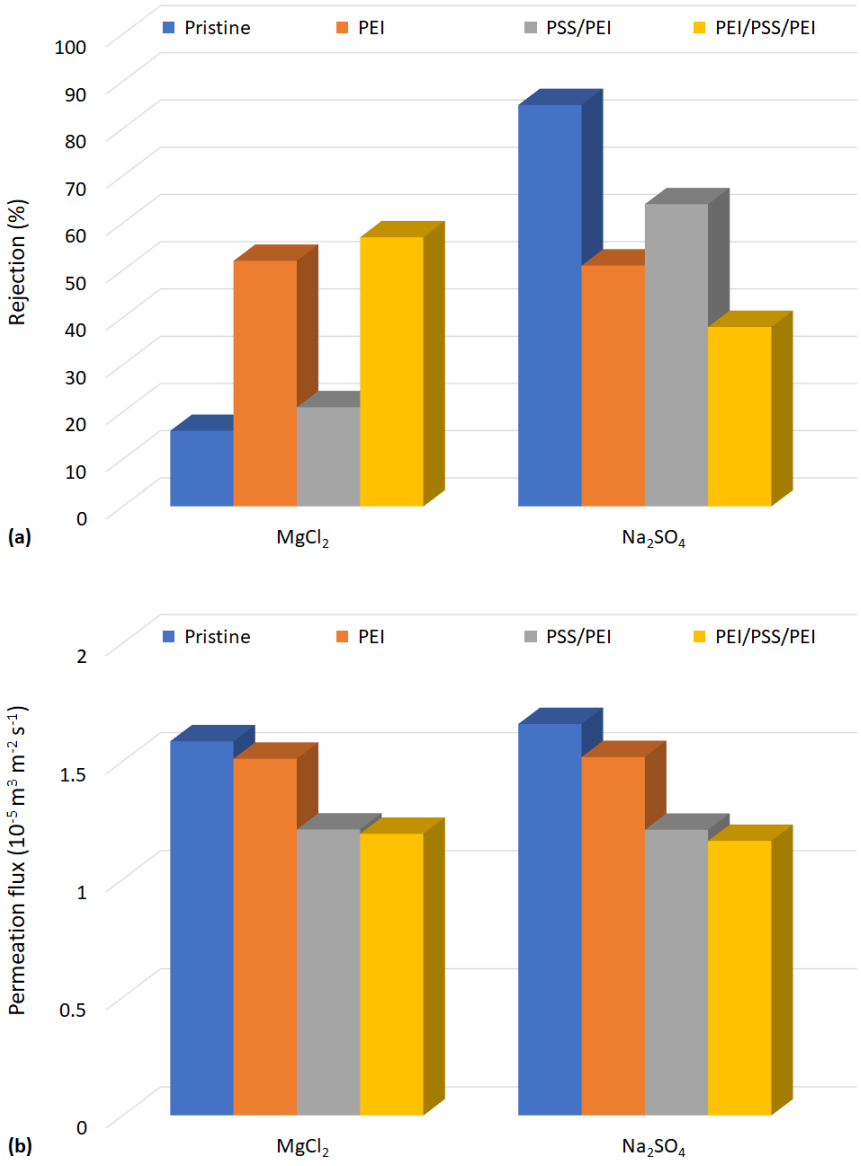

Fig. 11: Rejection (11a) and permeation flux (11b) at 15 bar of $MgCl_2$ and Na_2SO_4 measured with pristine and membranes modified by layer-by-layer electrospray deposition of PEI and PSS (PEI, PSS/PEI, PEI/PSS/PEI) {$C_{polymer} = 15 \times 10^{-1}$ mol/L and $V_{sprayed}$ = 12.5 µL/cm^2}

Concerning flux, it can be concluded that permeation is slightly more hindered when several layers are deposited, which has already been reported in literature [54]. However, it seems that

568 the decline involved by PSS deposition seems to affect more intensively permeation flux than
569 PEI deposition. Although surface hydrophilicity increases with PSS deposit, the decline in
570 permeation flux is in agreement with the notable increase of surface layer thickness observed
571 after electrospray deposition of PSS (Fig. 4f) and the corresponding increase in hydraulic
572 resistance.
573 It should be mentioned that the bulk permeability of the overall polymer film can show distinct
574 changes depending on the terminating layer, which is known as odd-even effects [45] and could
575 perhaps have an influence on observed permeability. However, a deeper investigation of this
576 phenomenon should have required to study a larger number of polymer layers. Finally, it should
577 be mentioned that ES depositions were implemented in the presence of KCl 10^{-3} mol/L to
578 comply with the same conditions as those required for electrokinetic characterization of the
579 surface. Nevertheless, it is well-known that background ionic strength strongly governs
580 polyelectrolyte layer structure and thus selectivity and permeability [55]. This specific point
581 appears to be an attractive prospect to extend this study.
582

IV. Conclusion

In this study, it was shown that electrospray deposition of polyelectrolytes is a suitable technique to tailor physicochemical properties of nanoporous membranes, and thus ion separation selectivity. This study highlighted that the deposition does not induce flux loss, and can even lead to a slight enhancement in specific conditions. It was also proved that this technique allows a notable adjustment of ion rejection, provided that the quantity of polymer is sufficient to induce a high solution viscosity, helping the deposit to withstand the shear stress inherent in cross-flow filtration. In particular, the charge of membrane surface can be strongly modified to either highly positive values of ζ-potential by spraying PEI or more negative values by spraying PSS (from -40 to +40 mV). This variation in membrane charge can lead to strong modification of separation selectivity induced by changes in electrostatic interactions between ions and membrane surface. It was especially shown that a positively charged superficial layer (PEI) induced an increase in rejection of divalent cation and a decrease in that of divalent anions. Superimposing many layers seems not to bring a substantial improvement compared with only one or two layers. Finally, the fact that surface hydrophilicity is notably increased by ES deposition of polymer, and especially PSS (from 60 up to 30°), bodes well for a real application since that tends to notably mitigate the membrane fouling by organic matter.

Acknowledgements

The authors would like to thank the region of Bourgogne Franche-Comté (Grant number: 2016Y-04563) for its financial support and especially for financing the Ph.D. thesis of Elizaveta Korzhova. The Institut de Science des Matériaux de Mulhouse (IS2M, UMR CNRS 7361), and especially Simon Gree and Aissam Airoudj, are acknowledged for performing IR spectroscopy. MIMENTO platform (FEMTO-ST, UMR CNRS 6174) and especially Roland Salut are also acknowledged for FIB-SEM images. Authors also thank Sandrine Monney (UTINAM platform) for performing AFM images and roughness analysis.

References

[1] R.W. Baker, Membrane technology and applications., John Wiley & Sons, Chichester, 2004.

[2] A. Efligenir, S. Déon, P. Fievet, C. Druart, N. Morin-Crini, G. Crini, Decontamination of polluted discharge waters from surface treatment industries by pressure-driven membranes: Removal performances and environmental impact, Chem. Eng. J., 258 (2014) 309-319.

[3] L.D. Nghiem, A.I. Schäfer, M. Elimelech, Role of electrostatic interactions in the retention of pharmaceutically active contaminants by a loose nanofiltration membrane, J. Membr. Sci., 286 (2006) 52-59.

[4] Y. Qi, L. Zhu, X. Shen, A. Sotto, C. Gao, J. Shen, Polythyleneimine-modified original positive charged nanofiltration membrane: Removal of heavy metal ions and dyes, Sep. Purif. Technol., 222 (2019) 117-124.

[5] B. Van der Bruggen, M. Mänttäri, M. Nyström, Drawbacks of applying nanofiltration and how to avoid them: A review, Sep. Purif. Technol., 63 (2008) 251-263.

[6] R. Zhang, Y. Liu, M. He, Y. Su, X. Zhao, M. Elimelech, Z. Jiang, Antifouling membranes for sustainable water purification: Strategies and mechanisms, Chem. Soc. Rev., 45 (2016) 5888-5924.

[7] W.J. Lau, S. Gray, T. Matsuura, D. Emadzadeh, J. Paul Chen, A.F. Ismail, A review on polyamide thin film nanocomposite (TFN) membranes: History, applications, challenges and approaches, Water Res., 80 (2015) 306-324.

[8] I. Sawada, R. Fachrul, T. Ito, Y. Ohmukai, T. Maruyama, H. Matsuyama, Development of a hydrophilic polymer membrane containing silver nanoparticles with both organic antifouling and antibacterial properties, J. Membr. Sci., 387-388 (2012) 1-6.

[9] C. Jiang, L. Tian, Y. Hou, Q.J. Niu, Nanofiltration membranes with enhanced microporosity and inner-pore interconnectivity for water treatment: Excellent balance between permeability and selectivity, J. Membr. Sci., 586 (2019) 192-201.

[10] M.H. Tajuddin, N. Yusof, I. Wan Azelee, W.N. Wan Salleh, A.F. Ismail, J. Jaafar, F. Aziz, K. Nagai, N.F. Razali, Development of Copper-Aluminum Layered Double Hydroxide in Thin Film Nanocomposite Nanofiltration Membrane for Water Purification Process, Frontiers in Chemistry, 7 (2019).

[11] V. Nayak, M.S. Jyothi, R.G. Balakrishna, M. Padaki, S. Déon, Novel modified poly vinyl chloride blend membranes for removal of heavy metals from mixed ion feed sample, J. Hazard. Mater., 331 (2017) 289-299.

[12] W. Wang, Y. Li, W. Wang, B. Gao, Z. Wang, Palygorskite/silver nanoparticles incorporated polyamide thin film nanocomposite membranes with enhanced water permeating, antifouling and antimicrobial performance, Chemosphere, (2019).

[13] Y. He, J. Liu, G. Han, T.S. Chung, Novel thin-film composite nanofiltration membranes consisting of a zwitterionic co-polymer for selenium and arsenic removal, J. Membr. Sci., 555 (2018) 299-306.

[14] V.S. Babu, M. Padaki, L.P. D'Souza, S. Déon, R. Geetha Balakrishna, A.F. Ismail, Effect of hydraulic coefficient on membrane performance for rejection of emerging contaminants, Chem. Eng. J., 334 (2018) 2392-2400.

[15] Y. Feng, M. Weber, C. Maletzko, T.S. Chung, Facile fabrication of sulfonated polyphenylenesulfone (sPPSU) membranes with high separation performance for organic solvent nanofiltration, J. Membr. Sci., 549 (2018) 550-558.

[16] S. Déon, Z. Koubaa, E. Korzhova, A. Airoudj, P. Fievet, V. Roucoules, Understanding the impact of poly(allylamine) plasma grafting on the filtration performances of a commercial polymeric membrane, Sep. Purif. Technol., 212 (2019) 30-39.

[17] Y. Qi, L. Zhu, X. Shen, A. Sotto, C. Gao, J. Shen, Polythyleneimine-modified original positive charged nanofiltration membrane: Removal of heavy metal ions and dyes, Sep. Purif. Technol., (2019) 117-124.

[18] J. Wang, R. He, X. Han, D. Jiao, J. Zhu, F. Lai, X. Liu, J. Liu, Y. Zhang, B. Van der Bruggen, High performance loose nanofiltration membranes obtained by a catechol-based route for efficient dye/salt separation, Chem. Eng. J., 375 (2019).

[19] Z.F. Gao, G.M. Shi, Y. Cui, T.S. Chung, Organic solvent nanofiltration (OSN) membranes made from plasma grafting of polyethylene glycol on cross-linked polyimide ultrafiltration substrates, J. Membr. Sci., 565 (2018) 169-178.

[20] S.J. Percival, L.J. Small, E.D. Spoerke, S.B. Rempe, Polyelectrolyte layer-by-layer deposition on nanoporous supports for ion selective membranes, RSC Adv., 8 (2018) 32992-32999.

[21] M. Ahmad, C. Tang, L. Yang, A. Yaroshchuk, M.L. Bruening, Layer-by-layer modification of aliphatic polyamide anion-exchange membranes to increase Cl–/SO42– selectivity, J. Membr. Sci., 578 (2019) 209-219.

[22] F. Fadhillah, S.M. Javaid Zaidi, Z. Khan, M. Khaled, F. Rahman, P. Hammond, Development of multilayer polyelectrolyte thin-film membranes fabricated by spin assisted layer-by-layer assembly, J. Appl. Polym. Sci., 126 (2012) 1468-1474.

[23] M. An, J.D. Hong, Surface modification of hafnia with polyelectrolytes based on the spin-coating electrostatic self-assembly method, Colloids and Surfaces A: Physicochemical and Engineering Aspects, 348 (2009) 301-304.

[24] S. Ilyas, R. English, P. Aimar, J.F. Lahitte, W.M. de Vos, Preparation of multifunctional hollow fiber nanofiltration membranes by dynamic assembly of weak polyelectrolyte multilayers, Colloids and Surfaces A: Physicochemical and Engineering Aspects, 533 (2017) 286-295.

[25] G. Zhang, X. Song, S. Ji, N. Wang, Z. Liu, Self-assembly of inner skin hollow fiber polyelectrolyte multilayer membranes by a dynamic negative pressure layer-by-layer technique, J. Membr. Sci., 325 (2008) 109-116.

[26] B. Su, T. Wang, Z. Wang, X. Gao, C. Gao, Preparation and performance of dynamic layer-by-layer PDADMAC/PSS nanofiltration membrane, J. Membr. Sci., 423-424 (2012) 324-331.

687 [27] Y. Zhao, C. Gao, B. Van der Bruggen, Technology-driven layer-by-layer assembly of a
688 membrane for selective separation of monovalent anions and antifouling, Nanoscale, 11
689 (2019) 2264-2274.

690 [28] Z. Zhao, S. Shi, H. Cao, Y. Li, B. Van der Bruggen, Layer-by-layer assembly of anion
691 exchange membrane by electrodeposition of polyelectrolytes for improved antifouling
692 performance, J. Membr. Sci., 558 (2018) 1-8.

693 [29] N. Joseph, P. Ahmadiannamini, R. Hoogenboom, I.F.J. Vankelecom, Layer-by-layer
694 preparation of polyelectrolyte multilayer membranes for separation, Polymer Chemistry, 5
695 (2014) 1817-1831.

696 [30] H. Tang, S. Ji, L. Gong, H. Guo, G. Zhang, Tubular ceramic-based multilayer separation
697 membranes using spray layer-by-layer assembly, Polymer Chemistry, 4 (2013) 5621-5628.

698 [31] M. Bruening, D. Dotzauer, Just spray it, Nat. Mater., 8 (2009) 449-450.

699 [32] J. Ma, H.M. Andriambololona, D. Quemener, M. Semsarilar, Membrane preparation by
700 sequential spray deposition of polymer PISA nanoparticles, J. Membr. Sci., 548 (2018) 42-49.

701 [33] P. Jin, C. Huang, Y. Li, J. Li, L. Wang, Fabrication of a superhydrophobic
702 poly(vinylidene fluoride) hollow fibre membrane by spray deposition, Micro and Nano
703 Letters, 13 (2018) 223-227.

704 [34] W. Ma, A. Soroush, T. Van Anh Luong, G. Brennan, M.S. Rahaman, B. Asadishad, N.
705 Tufenkji, Spray- and spin-assisted layer-by-layer assembly of copper nanoparticles on thin-
706 film composite reverse osmosis membrane for biofouling mitigation, Water Res., 99 (2016)
707 188-199.

708 [35] J.H. Kim, S.S. Shin, H.S. Noh, J.W. Son, M. Choi, H. Kim, Tailoring ceramic membrane
709 structures of solid oxide fuel cells via polymer-assisted electrospray deposition, J. Membr.
710 Sci., 544 (2017) 234-242.

711 [36] A.M. Chaparro, M.A. Folgado, P. Ferreira-Aparicio, A.J. Martín, I. Alonso-Álvarez, L.
712 Daza, Properties of catalyst layers for PEMFC electrodes prepared by electrospray deposition,
713 J. Electrochem. Soc., 157 (2010) B993-B999.

714 [37] S. Déon, B. Lam, P. Fievet, Application of a new dynamic transport model to predict the
715 evolution of performances throughout the nanofiltration of single salt solutions in
716 concentration and diafiltration modes, Water Res., 136 (2018) 22-33.

717 [38] S. Déon, P. Fievet, C. Osman Doubad, Tangential streaming potential/current
718 measurements for the characterization of composite membranes, J. Membr. Sci., 423–424
719 (2012) 413-421.

720 [39] Y. Lanteri, P. Fievet, S. Déon, P. Sauvade, W. Ballout, A. Szymczyk, Electrokinetic
721 characterization of hollow fibers by streaming current, streaming potential and electric
722 conductance, J. Membr. Sci., 411-412 (2012) 193-200.

723 [40] S. Déon, A. Escoda, P. Fievet, R. Salut, Prediction of single salt rejection by NF
724 membranes: An experimental methodology to assess physical parameters from membrane and
725 streaming potentials, Desalination, 315 (2013) 37-45.

[41] P. Dutournié, S. Déon, L. Limousy, Understanding the separation of anion mixtures by TiO2 membranes: Numerical investigation and effect of alkaline treatment on physicochemical properties, Chem. Eng. J., 363 (2019) 365-373.

[42] W.R. Bowen, A.O. Sharif, Transport through microfiltration membranes : particles hydrodynamics and flux reduction, J. Colloid Interface Sci., 168 (1994) 414-421.

[43] Q. Nan, P. Li, B. Cao, Fabrication of positively charged nanofiltration membrane via the layer-by-layer assembly of graphene oxide and polyethylenimine for desalination, Appl. Surf. Sci., 387 (2016) 521-528.

[44] R.M. DuChanois, R. Epsztein, J.A. Trivedi, M. Elimelech, Controlling pore structure of polyelectrolyte multilayer nanofiltration membranes by tuning polyelectrolyte-salt interactions, J. Membr. Sci., 581 (2019) 413-420.

[45] J. de Grooth, R. Oborný, J. Potreck, K. Nijmeijer, W.M. de Vos, The role of ionic strength and odd–even effects on the properties of polyelectrolyte multilayer nanofiltration membranes, J. Membr. Sci., 475 (2015) 311-319.

[46] C.P. Koutsou, S.G. Yiantsios, A.J. Karabelas, Direct numerical simulation of flow in spacer-filled channels: Effect of spacer geometrical characteristics, J. Membr. Sci., 291 (2007) 53-69.

[47] M.R. Moradi, A. Pihlajamäki, M. Hesampour, J. Ahlgren, M. Mänttäri, End-of-life RO membranes recycling: Reuse as NF membranes by polyelectrolyte layer-by-layer deposition, J. Membr. Sci., 584 (2019) 300-308.

[48] Ö. Tekinalp, S. Alsoy Altinkaya, Development of high flux nanofiltration membranes through single bilayer polyethyleneimine/alginate deposition, J. Colloid Interface Sci., 537 (2019) 215-227.

[49] B.W. Stanton, J.J. Harris, M.D. Miller, M.L. Bruening, Ultrathin, Multilayered Polyelectrolyte Films as Nanofiltration Membranes, Langmuir, 19 (2003) 7038-7042.

[50] X. Li, C. Liu, W. Yin, T.H. Chong, R. Wang, Design and development of layer-by-layer based low-pressure antifouling nanofiltration membrane used for water reclamation, J. Membr. Sci., 584 (2019) 309-323.

[51] J.-H. Zhu, B. Zhang, W.-W. Fang, X.-J. Lao, H. Yu, Characterization of amphoteric multilayered thin films by means of zeta potential measurements, Colloids Surf., B, 43 (2005) 1-6.

[52] S.U. Hong, R. Malaisamy, M.L. Bruening, Separation of Fluoride from Other Monovalent Anions Using Multilayer Polyelectrolyte Nanofiltration Membranes, Langmuir, 23 (2007) 1716-1722.

[53] Y. Huang, J. Sun, D. Wu, X. Feng, Layer-by-layer self-assembled chitosan/PAA nanofiltration membranes, Sep. Purif. Technol., 207 (2018) 142-150.

[54] S. Ilyas, S.M. Abtahi, N. Akkilic, H.D.W. Roesink, W.M. de Vos, Weak polyelectrolyte multilayers as tunable separation layers for micro-pollutant removal by hollow fiber nanofiltration membranes, J. Membr. Sci., 537 (2017) 220-228.

765 [55] W. Cheng, C. Liu, T. Tong, R. Epsztein, M. Sun, R. Verduzco, J. Ma, M. Elimelech,
766 Selective removal of divalent cations by polyelectrolyte multilayer nanofiltration membrane:
767 Role of polyelectrolyte charge, ion size, and ionic strength, J. Membr. Sci., 559 (2018) 98-
768 106.
769

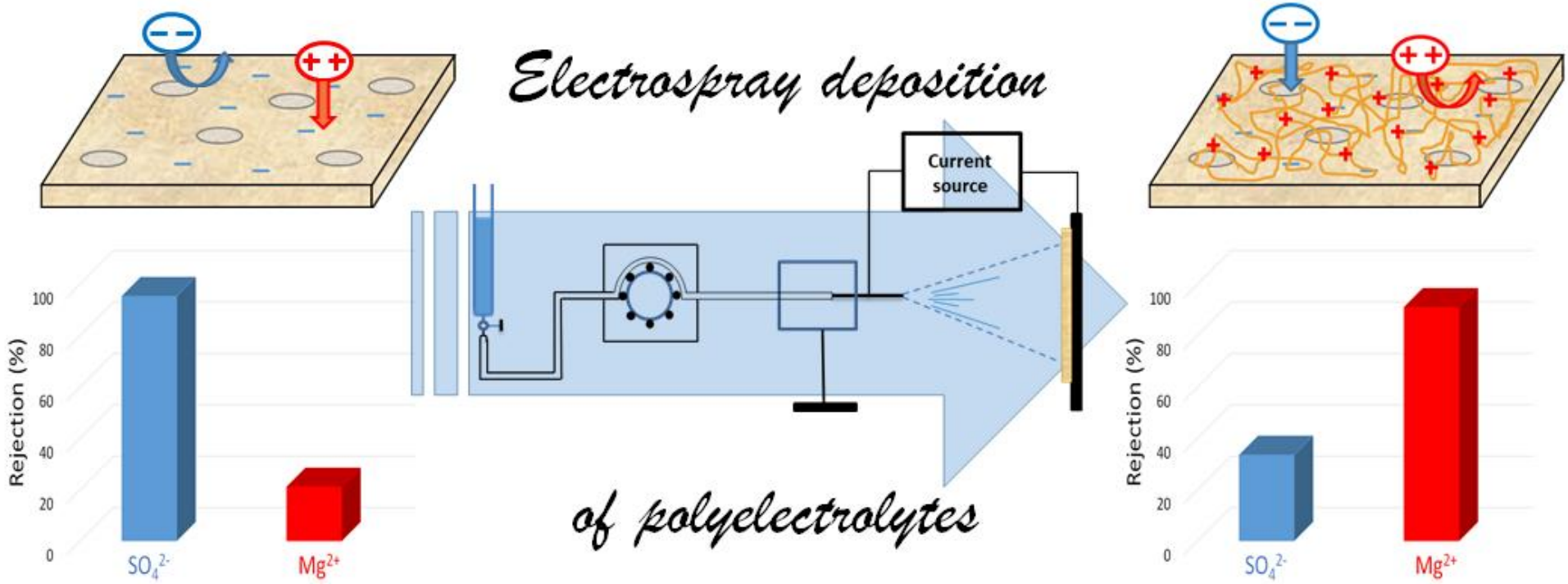
Electrospray deposition
of polyelectrolytes
Current source
Rejection (%)
100
80
60
40
20
0
SO_4^{2-}
Mg^{2+}
Rejection (%)
100
80
60
40
20
0
SO_4^{2-}
Mg^{2+}